Even−Odd Orientation and Chain-Length Effects in the Energy Exchange of Argon Collisions with Self-Assembled Monolayers

B. Scott Day and John R. Morris*

Department of Chemistry, Virginia Tech, Blacksburg, Virginia 24061

Received: February 11, 2003; In Final Form: May 13, 2003

Self-assembled monolayers (SAMs) of alkanethiols, $HS(CH_2)_{n-1}CH_3$ adsorbed on gold have been used to explore the dynamics of energy exchange and thermalization in high-energy gas−surface collisions. We find that the extent of thermalization and the fractional energy transferred to the surfaces during collisions with 80 kJ/mol Ar atoms are directly proportional to the alkyl chain length for $2 \leq n \leq 6$. The results suggest that long-range molecular motions involving up to 6 carbon atoms play the dominate role in controlling the dynamics of the gas−surface impact. In addition to the chain-length effect, alkanethiol monolayers with $n > 6$ show an oscillation in the amount of impulsively scattered atoms that depends on whether the chains consist of an even or an odd number of carbon atoms. The even−odd effect on the amount of impulsive scattering is associated with differences in the orientation of the terminal methyl group for the two classes of SAMs.

Introduction

The energy exchange dynamics of gas−surface collisions involving atomic gases and organic surfaces have been the subject of recent studies.[1−14] However, the often complex nature of organic surfaces has limited the number of detailed investigations into gas−surface energy transfer. A viable strategy for addressing this challenge is to employ self-assembled monolayers (SAMs) of alkanethiols on gold to create stable, well-ordered, and reproducible organic surfaces. SAMs are versatile enough to provide control over the surface functionality, the overall alkane chain structure, and the orientation of the outermost group on the surface. Using SAMs coupled with molecular beam scattering techniques, we have recently performed experiments that indicate that the hydrogen-bonding nature of molecules within model organic surfaces plays a role in determining the extent of gas−surface energy transfer and the propensity for impinging gases to thermally accommodate with the surface.[15,16]

The strategy of using self-assembled monolayers as well-ordered models for investigating gas−surface collisional dynamics has been employed in several experimental and theoretical studies. Naaman and co-workers[5,6] first employed this approach to reveal that concerted waving motions of alkane chains and hindered rotations of the end groups play a significant role in controlling gas−surface energy transfer. Using classical-trajectory simulations, Hase and co-workers explored the direct scattering and thermalization channels in collisions of rare-gases with alkanethiol self-assembled monolayers on gold.[7−10] Their studies also show that low-energy extended motions of monolayer alkane chains play the largest role in dissipating the energy of a gas−surface collision and the high-energy C−H motions play a minor role in the dynamics.[10] In addition to this work, several investigators including Cooks et al. have explored the characteristics of high-energy ionic collisions on model organic surfaces using a variety of ω-functionalized SAMs.[11,12] Hanley and co-workers have combined experimental and computational approaches to study the energy transfer of $SiMe_3^+$ on a 6-carbon alkanethiol SAM.[17,18] Their work shows that energy transfer to a surface is markedly greater for a monolayer-covered surface than it is for a bare gold surface and that penetration into the monolayer, even for greater than 10 eV ions, is limited to the topmost two-to-three layers of carbon atoms. Wysocki and co-workers,[13] and Bernasek et al.,[14] have also investigated the reaction dynamics of ion-surface scattering using SAMs. This set of work has provided important insight into how end-group orientation and the overall chain-length of a monolayer influences the ion-surface reaction dynamics.

The focus of the work presented here is to further the understanding of gas collisions on organic surfaces by exploring the impulsive energy transfer and thermalization of rare-gas atoms when they impact an *n*-alkanethiol self-assembled monolayer of the form $HS(CH_2)_{n-1}CH_3$ where $2 \leq n \leq 18$. It is now well-established that these molecules chemisorb onto Au(111) through a strong Au−S bond to form dense monolayers with an average intermolecular alkane chain separation of 5 Å, which produces an overall $(\sqrt{3} \times \sqrt{3})R30°$ lattice.[19−26] Optimal packing of the alkane chains occurs with the molecular axis tilted by approximately 30° with respect to the surface normal. The long-chain monolayers, with $n \geq 6$, have been shown to exhibit very high stability and crystalline-like long-range order characterized by a $c(4 \times 2)$ superlattice.[21−24] Although the short-chain monolayers have not been explored to the extent of the long-chain systems, several studies have shown that they readily form a complete monolayer of density and structure similar to that of the long-chain systems.[27−29] In general, alkanethiol self-assembled monolayers on gold have been demonstrated to be stable in ultrahigh vacuum (UHV) environments over time scales of several hours to several days.[21−24,30]

The *n*-alkanethiol SAMs, in conjunction with atomic-beam time-of-flight (TOF) scattering techniques, enable investigations into two key aspects of the collisional dynamics. First, our experiments explore the number of surface carbon atoms along an alkane chain that participate in the collision. Such studies are expected to lend insight into the importance of long-range molecular motions versus localized torsions and vibrations in controlling the outcome of a gas−surface collision. Second, as illustrated in Figure 1, the tilt of the monolayers with respect

* To whom correspondence should be addressed. E-mail: jrmorris@vt.edu.

10.1021/jp034349v CCC: $25.00
Published on Web 07/01/2003

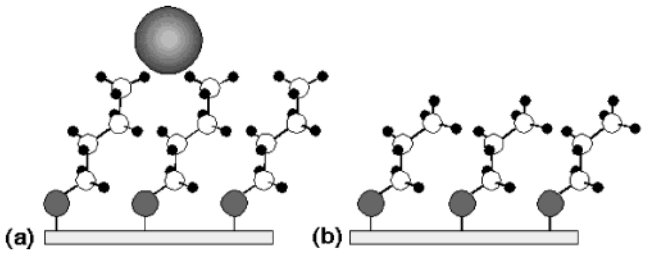

Figure 1. Schematic representation of the standing-phase for (a) an even-chain-length alkanethiol self-assembled monolayer and (b) an odd-chain-length alkanethiol self-assembled monolayer. Parts a and b illustrate the dependence of terminal group orientation on the even/odd nature of the alkanethiol chains. The sphere above the monolayer (a) corresponds to the van der Waals radius of an argon atom.

to the surface normal results in an n = even or n = odd dependence to the terminal C−C bond orientation.[19,31−33] Probing the influence of terminal group orientation on the scattering dynamics may help further elucidate the importance of localized C−C stretches, torsions, or bends in energy transfer and accommodation in gas−surface collisions.

Experimental Section

As in previous experiments performed in our group, the SAMs used in this study were prepared by spontaneous chemisorption of the alkanethiol from 1 mM ethanolic solutions onto clean Au surfaces.[15,16,34] We have performed experiments on gold substrates created by (1) evaporation onto heated mica (Molecular Imaging) and (2) evaporation onto Cr-coated glass slides (EMF Corp.). The gold-coated mica slides were flame-annealed prior to use to produce large Au (111) terraces, as verified in our group by scanning-tunneling microscopy studies. The gold-coated glass slides were cleaned in piranha solution (70/30 (v/v) mixture of H_2SO_4/H_2O_2) prior to use. Despite differences in the polycrystalline structure of the two gold surfaces,[35] the scattering results were found to have an insignificant dependence on the underlying substrate used for the monolayer.[15]

The chemicals used in this study were purchased from Aldrich without further purification. The clean gold slides were placed in the solutions for >12 h, rinsed with copious amounts of ethanol, dried under a stream of ultrahigh purity nitrogen, and then immediately transferred to the main UHV chamber ($\sim 7 \times 10^{-10}$ Torr) via a load-lock system. The total time between removal of the samples from the preparation solution and complete TOF data collection was ~60 min. We found the TOF spectra to be highly reproducible over this time period. The time the gold samples remained in solution did not have a measurable effect on the experimental results (over the range 1−24 h).

The experimental setup is similar to molecular beam scattering systems described previously.[36,37] High-energy atomic beams are created by expanding 2% Ar in H_2 at 700 Torr through a 0.05 mm diameter nozzle (General Valve). After passing through a 0.40 mm diameter conical skimmer located 6 mm from the nozzle, the beam enters a differential pumping stage where it collides with a mechanical chopper wheel. The slotted wheel, rotating at 300 Hz, produces approximately 60 μs pulses of gas that then pass through a 1.5 mm collimating aperture and into a final differential pumping stage. The final pumping stage is separated from the main UHV chamber by a 2.2 mm aperture through which the beam passes to produce a 1 cm spot size on the surface sample located in the main chamber, 36 cm from the nozzle. The molecular beam is characterized by a mass spectrometer located in the beam path directly behind the surface sample location. The peak energy of the 2% Ar in H_2 mixture is E_i = 80 kJ/mol (13 kJ/mol full width at half-maximum).

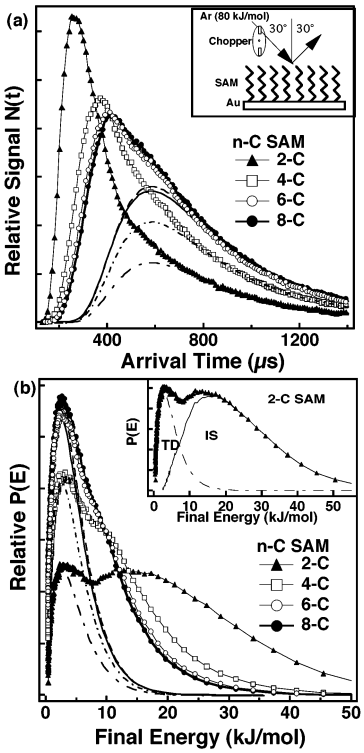

Figure 2. (a) Time-of-flight (TOF) spectra, $N(t)$, for 80 kJ/mol Ar scattering from $HS(CH_2)_{n-1}CH_3$ SAMs on Au with n = 2, 4, 6, and 8. The smooth curves are the Boltzmann distributions (at the temperature of the surface, T_s = 298 K) as determined from the $P(E)$ plots in part b. The inset of part a shows the experimental arrangement. Part b shows the data of part a converted to final translational energy distributions for Ar scattering from the n = 2, 4, 6, and 8 SAMs. The dashed lines are the Boltzmann distributions, and the inset illustrates the data deconvolution into the IS and TD components for the n = 2 monolayer.

The surface samples are laser-aligned so that the normal is in-plane and at $\theta_i = 30°$ to the molecular beam. A fraction of the atoms that scatter from the surface are intercepted by a doubly differentially pumped Extrel mass spectrometer oriented at 60° to the incident beam such that $\theta_f = 30°$. The ionizer of the mass spectrometer is positioned 29 cm from the surface and views a 1 cm spot size on the surface through two collimating apertures. The TOF distributions of the scattered atoms are determined by monitoring the mass spectrometer signal at m/z = 40 amu as a function of time. Each TOF scan is initiated when a slit of the chopper wheel passes a LED-photodiode arrangement that sends a voltage pulse to trigger a multichannel scalar (Ortec). The multichannel scalar integrates signal from the spectrometer in 2 μs intervals. Electronic and timing offsets, such as LED-photodiode trigger delays and ion flight times, are accounted for according to established protocols.[36,37]

The intensities and shapes of the TOF spectra were found to be highly stable and reproducible over the course of these studies. The stability in the experiments enables studies to be performed on many different surface samples under identical conditions, facilitating direct comparisons of TOF spectra on relative scales.

Results and Discussion

The closed triangle symbols of Figure 2a are the TOF data for the 80 kJ/mol Ar beam scattering from an n = 2 (2-C) SAM.

The high velocity peak that appears at early arrival times (~300 μs) corresponds to an impulsive scattering (IS) channel, and the broad component at later arrival times represents the molecules that have transferred enough energy to the surface to approach thermal equilibrium before exiting with a Boltzmann velocity distribution (thermal desorption, TD).[37] TOF data for the 4-, 6-, and 8-C SAMs are also presented in this figure. The IS and TD contributions to the scattering dynamics are determined by converting the TOF data, which are proportional to number density $N(t)$, into the $P(E)$ energy distributions shown in Figure 2b. The translational energy distributions are computed from the relations $E_f = (1/2)m_{Ar}(L/t)^2$ and $P(E_f) \sim t^2N(t)$, where t is the argon atom flight time over the distance, L. The translational energy distributions are separated into IS and TD by assigning the TD distribution to the component of $P(E_f)$ that falls within a Boltzmann distribution: $P_{TD}(E_f) = E_f\,(RT_{surf})^{-2}\exp(-E_f/RT_{surf})$.[3,38] The Boltzmann fits are shown for each data set. The IS contribution is assigned to the difference between $P(E_f)$ and $P_{TD}(E_f)$, constrained such that $P_{IS}(E_f) = 0$ at $E_f = RT_{surf} = 2.5$ kJ/mol. The inset of Figure 2b shows the IS and TD deconvolution for the 2-C SAM. As discussed below, the dynamics of gas−surface collisions are revealed through (a) analysis of the fractional energy transferred to the surface in the IS channel $(E_i - \langle E_{IS}\rangle)/E_i$, (b) the relative number of atoms that recoil (at $\theta_f = 30°$) with a thermal distribution of velocities (TD fraction), and (c) the relative number of atoms that recoil (at $\theta_f = 30°$) as part of a higher energy impulsive scattering channel.[3]

The TOF and $P(E)$ energy distributions of Figure 2 demonstrate that, as the chain-length decreases, the IS channel shifts to earlier arrival times (higher energy) and the TD intensity diminishes. We have scattered from a total of 15 surfaces ranging from $n = 2$ to 18 and the relative TD intensities, IS intensities, and fractional energy transfer in the IS channel for each surface are summarized in Figure 3.

Figure 3 reveals that as the total number of alkanethiol carbon atoms in the monolayer chains, n, increases from 2−6, the surface becomes a more effective energy sink for impinging atoms. Under the specular scattering conditions employed in this work ($\theta_i = \theta_f = 30°$), the TD intensity increases by a factor of 2, the IS intensity decreases by a factor of 3.4, and the fractional energy transfer increases from 0.71 to 0.84. However, the TD intensities and the energy transfer fractions are not sensitive to overall monolayer chain length for SAMs with greater than about 6 total carbon atoms. Figure 2a shows that the TOF distributions are nearly identical for the $n = 6$ and 8 surfaces. In contrast, the IS intensity is found to oscillate by approximately ±7% of the mean value depending on whether the alkane chains contain an even or an odd number of carbon atoms. Below, we discuss the effect that the chain length and the even−odd character of the SAMs have on the gas−surface scattering dynamics.

Alkane Chain Length Effect for $n \leq 6$. The angular distribution of Ar atoms that leave the surface after reaching thermal equilibrium (TD channel) likely consists of a cosine distribution according to the kinetic theory of gases and as revealed by several scattering experiments.[39−43] This cosine angular distribution for the TD channel is not expected to depend on surface alkane chain length. Although the data shown here represent only one final angle ($\theta_f = 30°$), the TD intensities reported in Figure 3a reveal the relative change in *overall* thermalization probability as a function of chain length. In contrast, the angular distribution of the impulsively scattered atoms has not yet been measured and is currently unknown for these systems. The IS intensities of Figure 3a are sensitive to changes in both the IS angular distribution *and* the overall number of Ar atoms that scatter impulsively from the surface. Interpretation of the trends in the IS intensity must take into account both effects. For cases where a decrease in IS intensity is balanced to some extent by an increase in TD intensity, such as the data for the short-chain SAMs, it is inferred that some of the atoms that would have scattered impulsively instead thermalize on the surface.

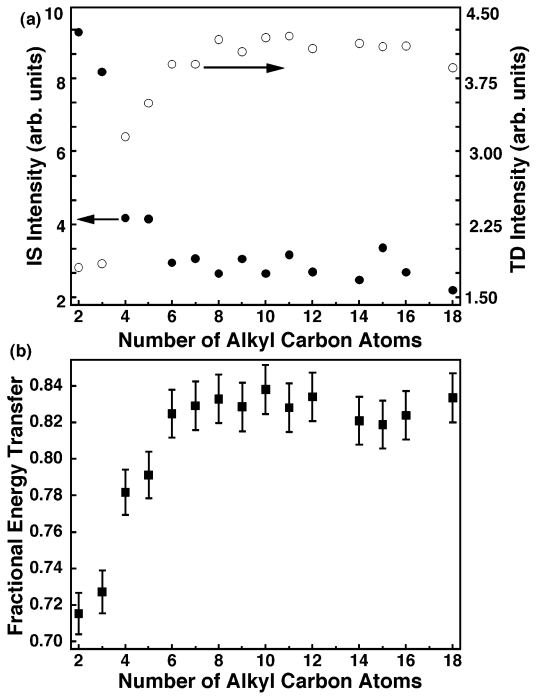

Figure 3. Summary of the scattering data for the entire range of SAMs from $n = 2$ to $n = 18$. Experiments were not performed on 13-C and 17-C SAMs. The solid symbols in part a are the relative IS intensities, and the open symbols are the TD intensities. The error bars are smaller than the size of the points. Part b is a plot of the fractional energy transfer, $(E_i - \langle E_{IS}\rangle)/E_i$, in the IS channel for each surface.

The nearly monotonic increase in the TD intensity, decrease in the IS intensity, and increase in the energy transfer fractions for SAMs with $2 \leq n \leq 6$ are likely the result of one or a combination of two factors: (a) a steady change in the surface structure with overall chain length or (b) a systematic increase in the available degrees-of-freedom within the surface as the chain length increases. The following discussion attempts to elucidate the relative importance of these two influences on the scattering dynamics.

It is likely that significant changes in the monolayer structure as the chain-length increases could alter the IS angular distributions as well as the total amount of impulsive scattering and thermalization. The structural characteristics of SAMs of the type used here are generally grouped into two categories: (1) a "striped" phase that occurs at low coverage and (2) a full-coverage high-density standing phase. Poirier et al. have used scanning-tunneling microscopy to investigate the molecular-level structure of butanethiol monolayers on gold.[44−46] Their results, along with the XPS work of Leggett and co-workers[47] and the IR measurements of Rowntree et al.,[29] indicate that 4-carbon alkanethiols initially form a full-coverage high-density monolayer on the surface under the preparation conditions employed in the work presented here. Desorption of alkanethiols from this high-density monolayer in UHV has been shown to be slow, occurring on the time-scale of days, and the longer chain SAMs

have even greater stability. Our TOF data collection is complete in less than 1 h after insertion into the chamber and the distributions are found to be highly consistent over a 5-h period. Therefore, it is reasonable to assume that the experiments presented here are all performed on the full-coverage standing phase of the SAMs for both short-chain and long-chain systems.

Despite similar coverage, the short-chain SAMs can differ structurally from the long-chain monolayers. Most significantly, the short-chain systems may form a 2-dimensional liquidlike phase, as opposed to the solid crystalline-like phase formed by long-chain monolayers.[44−46] Interestingly, the phase transition from the liquid phase to the crystalline phase occurs for chains with 6−7 carbon atoms,[48] which coincides with the point at which the TD fractions of Figure 3 cease to depend on chain length. However, previous structural studies have established that annealing even short-chain *n*-alkanethiol SAMs orders the monolayers into the crystalline superlattice.[27] Because we have found that annealing, which re-orders the monolayers, has no measurable influence on the energy transfer dynamics,[34] we suggest that trends presented here are not due solely to changes in surface order as a function of *n*. Therefore, we turn to alternative explanations for the observed scattering dynamics.

An alternative explanation for our results is that the available energetic degrees-of-freedom within the surface increase with chain length and that as many as 6-carbon atoms along an individual chain participate in dissipating the energy of the gas−surface collisions. This explanation is consistent with the expected time scales for the impulsive gas−surface collision and the rate at which energy propagates along a hydrocarbon chain. Molecular dynamics simulations indicate that for rare-gas collisions with an organic monolayer, the interaction time is about 0.5−1 ps.[7] During this short time, a limited group of atoms in the monolayer can respond collectively, regulated by the speeds of accessible inter- and intramolecular motions.[3] An estimate of the rate of energy propagation away from the point of collision is the speed of sound along an alkane chain. This speed has been estimated to be ∼15 Å/ps for a 30-carbon alkane chain,[50] yielding propagation distances within the monolayer of 7.5−15 Å for the 0.5 ps to 1 ps interaction time. Given a C−C bond length of 1.53 Å,[51] these distances indicate that 5−10 carbon atoms along the alkane chains can participate in the gas−surface collision. Indeed, our results show that 6 or more atoms are needed to dissipate the collisional energy. The picture that emerges from this discussion is that long-range molecular motions such as C−C stretches, bends, wags, and possibly conformational changes[10] play the most important role in determining the extent of energy transfer and thermalization in collisions of gases with these organic thin films.

Odd−Even Effect for $n > 6$. For SAMs with $n > 6$, we find that the impulsive energy transfer and the extent of thermalization on the surface are independent of overall chain length. However, the amount of impulsive scattering at the specular angle ($\theta_i = \theta_f = 30°$) is found to depend on whether the alkane chains contain an even or an odd number of carbon atoms. Figure 4 shows a direct comparison on a relative scale of the TOF distributions for 80 kJ/mol Ar scattering from an $n = 8$ and an $n = 9$ monolayer. The TOF and $P(E)$ distributions reveal that the Boltzmann components for scattering from the two surfaces are indistinguishable. As discussed above, because the angular distribution of thermally desorbing atoms is expected to be the same for both surfaces, it follows that the total number of Ar atoms that reach thermal equilibrium is nearly the same for both chain-length monolayers. The main difference in the scattered distributions comes from the impulsive scattering

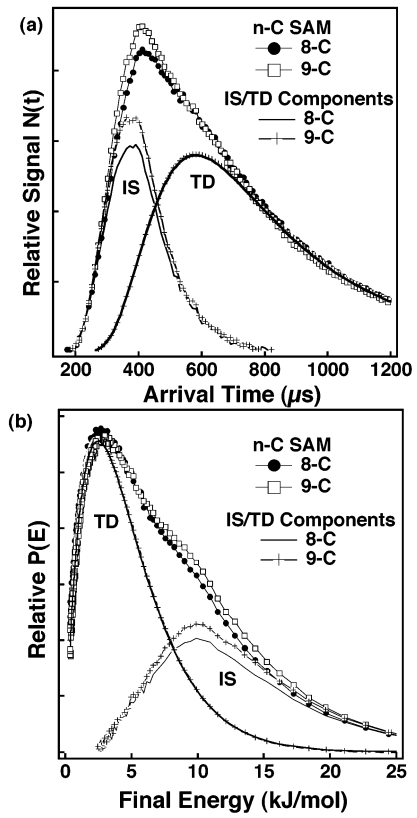

Figure 4. (a) TOF distributions for 80 kJ/mol Ar scattering from $HS(CH_2)_8CH_3$ and $HS(CH_2)_9CH_3$ SAMs along with the IS and TD contributions. (b) $P(E)$ distributions for the same 9-C and 8-C SAMs of part a.

component. The IS intensity for Ar scattering from the 9-C monolayer is found to be measurably larger than the IS intensity for scattering from the 8-C monolayer. Figure 3 shows that this trend holds for the entire range of $n > 6$ monolayers studied, indicating that there is greater propensity for Ar to scatter impulsively to the specular angle of 30° for an $n =$ odd than for an $n =$ even monolayer. Because the increase/decrease in the IS intensities are not balanced by a decrease/increase in the TD channel, the even/odd oscillations are most likely due to a dependence of the IS angular distributions on the even/odd character of the monolayer.

As in the previous discussion of the chain-length effect on scattering, the phenomena responsible for the even−odd effect is likely one or a combination of two possibilities: structural influences and available degrees-of-freedom. The well-documented structural difference between the long-chain monolayers is that the orientation of the terminal C−C bond alternates from predominately parallel to perpendicular to the surface depending on whether the total number of carbon atoms is odd or even, respectively (see Figure 1).[19,31−33] Differences in orientation may influence the ability of argon to excite terminal C−H stretches, C−C stretches, methyl torsions, and C−C−C bends. Minor differences in the amount of impulsive energy transfer between the even and odd surfaces would affect the final parallel momentum of the atoms in the IS channel thereby altering the angular distribution. Alternatively, one may speculate that slight differences in the surface roughness could lead to the observed trends.[1,2,52,53]

Simple ball-and-stick models of the type shown in Figure 1 illustrate that the second carbon from the methyl-terminal group is actually closer to the outermost layer of the surface for the odd-chain-length SAMs than it is for the even-chain monolayers.

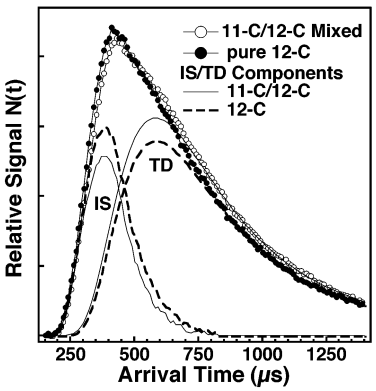

Figure 5. TOF distributions for Ar scattering from a SAM created in a solution composed of a 1:1 mixture of 11-C and 12-C alkanethiols (open symbols) and the TOF distribution for Ar scattering from a pure 12-C SAM.

In this picture, the n = odd monolayers may appear slightly less rough on the atomic scale, thereby reducing the amount of out-of-plane impulsive scattering relative to the even-chain monolayers.[1,2,52,53] We have attempted to explore how minor differences in surface roughness affect the IS and TD intensities by creating a SAM composed of approximately a 1:1 mixture of 11-C and 12-C alkanethiols. Figure 5 is a comparison of the TOF distributions for 80 kJ/mol Ar atoms scattering from a pure dodecanethiol SAM and the intentionally roughened mixed SAM. The comparison shown in Figure 5 demonstrates, as expected from previous work,[1,2,52,53] that the TD intensity is greater on the mixed (rough) SAM. We find that many of the atoms that scatter impulsively on the smooth surface instead undergo additional collisions to dissipate their excess energy and approach thermal equilibrium on the mixed surface. Although we have not quantitatively determined the surface structures or degree of roughness of the mixed SAM, the data shows that a decrease in the IS channel due to roughness is balanced, to some extent, by an increase in the TD intensity.

Because what may be a minor change in surface roughness is found to have a measurable influence on the TD channel, the even−odd effect may not be due to changes in the atomic scale roughness of the two monolayers. A more likely explanation for the observed even−odd effect is that slight differences in the impulsive energy transfer for even and odd surfaces lead to differences in the final parallel momentum and, hence, different IS angular distributions for impulsively scattered atoms. These differences should also be evident in the fractional energy transfer plots of Figure 3a, but the relatively large error bars in the data may preclude its observation. Although the above explanation for the even−odd effect is consistent with the experimental results presented here, there is currently not sufficient evidence to rule out other possibilities, and further experiments are required. In particular, angle-resolved TOF studies and classical trajectory simulations, both of which are underway, are expected to more fully elucidate the scattering dynamics.

Summary

Molecular beam scattering of high-energy Ar from self-assembled monolayers composed of *n*-alkanethiols ranging from 2 to 18 total carbon atoms have provided insights into the impulsive energy transfer and thermalization dynamics of gas collisions on organic surfaces. In particular, the findings indicate that, as the total number of alkanethiol carbon atoms in the monolayer chains increases from 2 to 6, the surfaces become progressively less rigid leading to greater energy transfer in the impulsive scattering channel accompanied by a larger extent of thermalization on the surface. Because this chain-length effect cannot be directly related to changes in surface structure as the number of carbon atoms increase, it is attributed to the importance of long-range motions along the alkane chains. It appears that up to 6 carbon atoms participate in the dynamics of the gas−surface collisions. In contrast to short-chain systems, the amount of thermalization and the extent of impulsive energy transfer are independent of chain length for SAMs constructed from alkanethiols with 6−18 carbon atoms along the chain. However, the scattered intensity of atoms in the impulsive channel are found to oscillate about a mean value depending on whether the alkane chains contain an even or an odd number of carbon atoms. It is speculated that small changes in the angular distribution of atoms scattered in this channel are responsible for the experimental observations. These changes may be the result of small differences in the atomic-scale roughness or the ability to couple energy into the various surface modes.

Acknowledgment. Funding was provided by the National Science Foundation (CAREER Award No. CHE-94269). We also thank Gwen Davis and James Lohr for valuable help in instrument construction.

References and Notes

(1) King, M. E.; Nathanson, G. M.; Hanning-Lee, M. A.; Minton, T. K. *Phys. Rev. Lett.* **1993**, *70*, 1026.
(2) King, M. E.; Saecker, M. E.; Nathanson, G. M. *J. Chem. Phys.* **1994**, *101*, 2539.
(3) Saecker, M. E.; Nathanson, G. M. *J. Chem. Phys.* **1993**, *99*, 7056.
(4) Zhang, J.; Garton, D. J.; Minton, T. K. *J. Chem. Phys.* **2002**, *117*, 6239.
(5) Cohen, S. R.; Naaman, R.; Sagiv, J. *Phys. Rev. Lett.* **1987**, *58*, 1208.
(6) Paz, Y.; Naaman, R. *J. Chem. Phys.* **1991**, *94*, 4921.
(7) Bosio, S. B. M.; Hase, W. L. *J. Chem. Phys.* **1997**, *107*, 9677.
(8) Yan, T.; Hase, W. L. *Phys. Chem. Chem. Phys.* **2000**, *2*, 901.
(9) Yan, T.; Hase, W. L.; Barker, J. R. *Chem. Phys. Lett.* **2000**, *329*, 84.
(10) Yan, T.; Hase, W. L. *J. Phys. Chem. B.* **2002**, *106*, 8029.
(11) Wade, N.; Evans, C.; Pepi, F.; Cooks, R. G. *J. Phys. Chem. B* **2000**, *104*, 11230.
(12) Cooks, G. G.; Ast, T.; Pradeep, T.; Wysocki, V. *Acc. Chem. Res.* **1994**, *27*, 316.
(13) V. Angelico, J.; Mitchell, S. A.; V.; Wysocki, H. *Anal. Chem.* **2000**, *72*, 2603.
(14) Wolf, K. V.; Cole, D. A.; Bernasek, S. L. *Langmuir* **2001**, *17*, 8254.
(15) Shuler, S. F.; Davis, G. M.; Morris, J. R. *J. Chem. Phys.* **2001**, *116*, 9147.
(16) Day, B. S.; Davis, G. M.; Morris, J. R. *Anal. Chem. Acta* **2003** in press.
(17) Schultz, D. G.; Wainhaus, S. B.; Hanley, L.; de Sainte Claire, P.; Hase, W. L. *J. Chem. Phys.* **1997**, *106*, 10337.
(18) Wainhaus, S. B.; Lim, H.; Schultz, D. G.; Hanley, L. *J. Chem. Phys.* **1997**, *106*, 10329.
(19) Nuzzo, R. G.; Dubois, L. H.; Allara, D. L. *J. Am. Chem. Soc.* **1990**, *112*, 558.
(20) Ulman, A. *Chem. Rev.* **1996**, *96*, 1533.
(21) Camillone, N., III.; Chidsey, C. E. D.; Liu, G. Y.; Putvinski, T. M.; Scoles, G. *J. Chem. Phys.* **1991**, *94*, 8493.
(22) Camillone, N.; Chidsey, C. E. D.; Liu, G. Y.; Scoles, G. *J. Chem. Phys.* **1993**, *98*, 3503.
(23) Camillone, N., III.; Eisenberger, P.; Leung, T. Y. B.; Schwartz, P.; Scoles, B. *J. Chem. Phys.* **1994**, *101*, 11031.
(24) Camillone, N.; Leung, T. Y. B.; Scoles, G. *Surf. Sci.* **1997**, *373*, 333.
(25) Touzov, I.; Gorman, C. B. *J. Phys. Chem. B* **1997**, *101*, 5263.
(26) Gorman, C. B.; He, Y.; Carroll, R. L. *Langmuir* **2001**, *17*, 5324.
(27) Danisman, M. F.; Casalis, L.; Bracco, G.; Scoles, G. *J. Phys. Chem. B* **2002**, *106*, 11771.
(28) Vargas, M. C.; Giannozzi, P.; Selloni, A.; Scoles, G. *J. Phys. Chem. B* **2001**, *105*, 9509.

(29) Truong, K. D.; Rowntree, P. A. *J. Phys. Chem.* **1996**, *100*, 19917.
(30) Darling, S. B.; Rosenbaum, A. W.; Wang, Y.; Sibener, S. J. *Langmuir* **2002**, *18*, 7462.
(31) Bryant, M. A.; Pemberton, J. E. *J. Am. Chem. Soc.* **1991**, *113*, 8284.
(32) Laibinis, P. E.; Nuzzo, R. G.; Whitesides, G. M. *J. Phys. Chem.* **1991**, *96*, 5097.
(33) Laibinis, P. E.; Whitesides, G. M.; Allara, D. L.; Tao, Y. T.; Parikh, A. N.; Nuzzo, R. G. *J. Am. Chem. Soc.* **1991**, *113*, 7152.
(34) Day, B. S.; Shuler, S. F.; Ducre, A.; Morris, J. R. *J. Chem. Phys.* submitted.
(35) Touzov, I.; Gorman, C. B. *J. Phys. Chem. B* **1997**, *101*, 5263.
(36) Ceyer, S. T.; Gladstone, D. J.; McGonigal, M.; Schulberg, M. T. Molecular Beams: Probes of the Dynamics of Reactions on Surfaces. In *Physical Methods of Chemistry*, 2 ed.; Wiley: New York, 1988.
(37) Miller, D. R. In *Atomic and Molecular Beam Methods, Vol. 1*; Scoles, G., Eds.; Oxford University Press: New York, 1988.
(38) Nathanson, G. M.; Morgan, J. A. *J. Chem. Phys.* **2001**, *114*, 1958.
(39) Fisher, S. S.; Hagena, O. F.; Wilmoth, R. G. *J. Chem. Phys.* **1968**, *49*, 5035.
(40) Auerbach, D. J.; Comsa, G.; Poelsema, B.; Asscher, M.; Somorjai, G. *Atomic and Molecular Beam Methods*; Scoles, G., Ed.; Oxford University Press: New York, 1988; Vol. 1.
(41) Harris, J.; Weinberg, W. H. *Dynamics of Gas−Surface Interactions*; Rettner, C. T.; Ashfold, M. N. R. Eds. Royal Society of Chemistry: Cambridge, 1991.
(42) Barker, J. A.; Auerbach, D. J. *Surf. Sci. Rep.* **1985**, *4*, 1.
(43) Wenaas, E. P. *J. Chem. Phys.* **1971**, *4*, 376.
(44) Poirier, G. E.; Tarlov, M. J.; Rushmeier, H. E. *Langmuir* **1994**, *10*, 3383.
(45) Poirier, G. E.; Tarlov, M. J. *Langmuir* **1994**, *10*, 2853.
(46) Poirier, G. E.; Tarlov, M. J. *J. Phys. Chem.* **1995**, *99*, 10966.
(47) Hutt, D. A.; Leggett, G. J. *Langmuir* **1997**, *13*, 3055.
(48) Porter, M. D.; Bright, T. B.; Allara, D. L.; Chidsey, C. E. D. *J. Am. Chem. Soc.* **1987**, *109*, 3559.
(49) Fenter, P.; Eisenberger, P.; Liang, K. S. *Phys. Rev. Lett.* **1993**, *70*, 2447.
(50) Champion, J. V.; Jackson, D. A. *Mol. Phys.* **1976**, *31*, 1159.
(51) Bumm, L. A.; Arnold, J. J.; Charles, L. F.; Dunbar, T. D.; Allara, D. L.; Weiss, P. S. *J. Am. Chem. Soc.* **1999**, *121*, 8017.
(52) Tribe, L.; Manning, M.; Morgan, J. A.; Stephens, M. D.; Ronk, W. R.; Treptow, E.; Nathanson, G. M.; Skinner, J. L. *J. Phys. Chem. B* **1998**, *102*, 206.
(53) Ronk, W. R.; Kowalski, D. V.; Manning, M.; Nathanson, G. M. *J. Chem. Phys.* **1996**, *104*, 4842.